Original Research Article

piR-36249 and DHX36 together inhibit testicular cancer cells progression by upregulating OAS2

Qianqian Wang [a,b,1], Peize Chen [b,1], Xiaorong Wang [c,1], Yueming Wu [b], Kaiguo Xia [d], Xiangyu Mu [a], Qiang Xuan [a], Jun Xiao [a], Yaohui He [e], Wen Liu [e], Xiaoyuan Song [a,b,*], Fei Sun [f,**]

[a] Department of Urology, The First Affiliated Hospital of University of Science and Technology of China, Division of Life Sciences and Medicine, University of Science and Technology of China, Hefei, Anhui, 230001, China
[b] Hefei National Laboratory for Physical Sciences at the Microscale, MOE Key Laboratory for Cellular Dynamics, CAS Key Laboratory of Brain Function and Disease, School of Life Sciences, Division of Life Sciences and Medicine, University of Science and Technology of China, Hefei, Anhui, 230027, China
[c] Center for Reproductive Medicine, Affiliated Maternity and Child Health Care Hospital of Nantong University, Nantong, Jiangsu, 226018, China
[d] Department of Urology, The First Affiliated Hospital of Anhui Medical University, Hefei, 230022, China
[e] School of Pharmaceutical Science, Fujian Provincial Key Laboratory of Innovative Drug Target Research, Xiamen University, Xiamen, Fujian, 361102, China
[f] Department of Urology & Andrology, Sir Run Run Shaw Hospital, Zhejiang University School of Medicine, Hangzhou, Zhejiang, 310016, China

ABSTRACT

Background: PIWI-interacting RNAs (piRNAs) are a class of noncoding RNAs originally reported in the reproductive system of mammals and later found to be aberrantly expressed in tumors. However, the function and mechanism of piRNAs in testicular cancer are not very clear.
Methods: The expression level and distribution of piR-36249 were detected by RT-qPCR and immunofluorescence staining assay. Testicular cancer cell (NT2) progression was measured by CCK8 assay, colony formation assay and wound healing assay. Cell apoptosis was assessed by flow cytometry and western blot. RNA sequencing and dual-luciferase reporter assay were conducted to identify the potential targets of piR-36249. The relationship between piR-36249 and *OAS2* or DHX36 was confirmed using overexpression assay, knockdown assay, pull-down assay and RIP assay.
Results: piR-36249 is significantly downregulated in testicular cancer tissues compared to tumor-adjacent tissues. Functional studies demonstrate that piR-36249 inhibits testicular cancer cell proliferation, migration and activates the cell apoptosis pathway. Mechanically, we identify that piR-36249 binds to the 3′UTR of 2′-5′-oligoadenylate synthetase 2 (*OAS2*) mRNA. *OAS2* has been shown in the literature to be a tumor suppressor modulating the occurrence and development of some tumors. Here, we show that *OAS2* knockdown also promotes testicular cancer cell proliferation and migration. Furthermore, piR-36249 interacts with DHX36, which has been reported to promote translation. DHX36 can also bind to *OAS2* mRNA, and knockdown of DHX36 increases *OAS2* mRNA but downregulates its protein, indicating the enhancing effect of DHX36 on OAS2 protein expression.
Conclusion: All these data suggest that piR-36249, together with DHX36, functions in inhibiting the malignant phenotype of testicular cancer cells by upregulating OAS2 protein and that piR-36249 may be used as a suppressor factor to regulate the development of testicular cancer.

1. Introduction

PIWI-interacting RNAs (piRNAs) are single-stranded noncoding RNAs with a length of 23–36 nucleotides (nt) [1]. piRNAs are abundantly enriched in germ cells and function in the regulation of spermatogonia self-renewal, mitotic spermatocytes and the development of testicular carcinoma [2,3]. piRNAs exhibit tissue-specific expression patterns in human tissues and associate with PIWI proteins

to be involved in important signaling pathways at the transcriptional or posttranscriptional levels [4–7]. Recently, several model studies have identified a strong link between the abnormal expression of piRNAs and malignant phenotype (including initiation, proliferation, and metastasis) of multiple cancers such as gastric [8], breast [9,10], kidney [11,12], colon [13–15], and lung cancers [16,17]. Thus, piRNAs could be potential diagnostic tools and therapeutic targets for cancers.

Testicular cancer is a rare tumor in the general population but one of the most common malignancies in men aged 15–44 years [18–20], and its incidence has risen in Western countries over the past two decades. More than 90% of testicular neoplasms originate from germ cells [21]. Testicular germ cell tumor (TGCT) is believed to arise from failure of normal maturation of gonocytes. TGCTs are divided into seminomas and nonseminomas [22]. Studies have found that primary TGCTs can metastasize to retroperitoneal lymph nodes [23], the brain [24] and the heart [25]. This reflects the aggressive biological characteristics of testicular tumors and the difficulties and challenges faced by the current treatment of testicular cancer. The side effects of TGCT treatment on other organs will become a long-term risk factor for the survival of TGCT patients. It has been reported that renal disease in TGCT patients is associated with chemotherapy [26]. In addition, TGCTs have significant heritability, and the relative familial risk is much higher than that of most other cancers. Research groups have studied the genetic risk factors for TGCTs and identified abnormally expressed genes associated with TGCTs [27–29]. These studies showed that noncoding RNAs can act as tumor suppressor genes or oncogenes to regulate gene expression in TGCTs and thus can serve as potential diagnostic biomarkers and develop novel therapies based on controlling gene expression [30,31]. Since piRNAs play important roles in most cancers, we hypothesized that piRNAs might as potential mediators in the oncogenesis and progression of testicular cancer.

Here, our results clarified the function and underlying mechanisms of piR-36249 in testicular cancer cells. piR-36249 was drastically downregulated in testicular cancer tissues. Furthermore, piR-36249 and DHX36 interact with the *OAS2* mRNA 3′UTR to promote *OAS2* expression and inhibit testicular cancer cell proliferation, migration and enhance apoptosis. Our findings will contribute to a better understanding of the function and mechanism of piRNAs in the development and progression of testicular cancer cells.

2. Materials and methods

2.1. Human testicular cancer samples

The human testicular cancer samples were postoperative specimen during Urological surgery and obtained from The First Affiliated Hospital of Anhui Medical University (Hefei, China). All samples were submitted to Surgical Pathology for microscopic examination. We collected postoperative specimens (paired testicular germ cell tumor tissue and normal testicular tissue, n = 3 each). The total RNAs of fresh tumor sample were extracted using TRIzol™ Reagent and RT-qPCR analysis to identify expression level of piR-36249. All patients signed informed consent documents approving the use of their tissues for research purposes (Permit number: 20170354).

2.2. Cell culture and transfection

The human seminoma cell line TCAM2 was kindly provided by Dr. Yupeng Wu (Bengbu Medical College, Bengbu, China) and immersed in culture medium (DMEM, Invitrogen, 61100-061) containing fresh 10% fetal bovine serum (FBS, EVERY GREEN, 70220-8611), 1% penicillin–streptomycin (PS, WISENT, 450-115-EL) and 1% ʟ-glutamine. The human teratocarcinoma cell line NT2, mouse testicular Leydig cell line TM3, and mouse spermatogonial cell line GC1 were grown in DMEM with 10% FBS (ExCell Bio, FSS500), 1% PS and 1% ʟ-glutamine. Cells were cultured in a cell incubator with 5% CO_2 at 37 °C.

For cell transfection assay, 6×10^4 cells were seeded into twelve-well plates and grown to 60% confluence. piR-36249 mimics, inhibitor, and scrambled siRNA oligonucleotides were transfected into NT2 cells, respectively, using transfection reagent (INTERFERin, Polyplus, 409-10) according to the manufacturer's instructions. RNA oligonucleotides were made in GenePharma (Shanghai, China). The sequences of all oligonucleotides are listed in Supplemental Table S1.

2.3. RNA isolation, reverse transcription and quantitative PCR (RT-qPCR)

RNA extraction, reverse transcription and quantitative real-time PCR (qPCR) experiments were performed as previously described [32]. We used TRIzol™ Reagent and isolated RNA component from testicular cancer tissue or cell lines. 1% agarose gel electrophoresis was used to evaluate RNA sample quality and concentration was detected by micro spectrophotometer (Nano300, ALLSHENG, China). Reverse transcription and qPCR for piR-36249 and endogenous control U6 snRNA were performed using miRNA quantitation kit (GenePharma, E22003) according to the instructions strictly. The relative expression of the candidate genes was calculated to the endogenous reference *GAPDH* mRNA and *U6* RNA using the 2DeltaDeltaCt method. The specific information of the RT-qPCR primers are shown in Supplemental Materials Table S1.

2.4. Nuclear and cytoplasmic separation

NT2 cells and TCAM2 cells were fractionated into the nucleus and cytoplasm, and total RNA and protein were isolated. One million cells were prepared and resuspended gently in 500 μL ice cold RSB-100 solution (10 mM Tris-HCl pH 7.4, 100 mM NaCl, 25 mM MgCl₂, 40 μg/mL digitonin). The cells were transferred immediately and lysed on ice for 3–5 min on ice. Then, cell lysate was centrifuged at 2000×g for 8–10 min at 4 °C. The supernatant (250 μL for RNA and 50 μL for protein) was collected for the cytoplasmic fraction, and the pellet was resuspended in 500 μL of RSB-100 solution for the nuclear fraction, followed by the operations described above. Protein samples were identified by Western blot assay. RNA samples were used for RT-qPCR analysis.

2.5. Western blot assay

Ten million cells were collected and lysed in 1 mL RIPA buffer (150 mM NaCl, 1 mM EDTA, 1% Triton X-100, 1% SDS, 1% sodium deoxycholate, 50 mM Tris-HCl pH 7.4) supplemented with fresh protease inhibitor cocktail on ice for 1 h. The protein samples were harvested by centrifuged at 16,000×g for 10 min at 4 °C, denatured with 2 × SDS loading buffer (0.2% bromophenol blue, 10% β-mercaptoethanol, 20% glycerol, 10% DTT, 125 mM Tris-HCl pH 6.8, 4% SDS) under heat treatment. Protein samples were added to the groove in order and separated by 10% SDS-PAGE. Next, the target proteins were transferred to PVDF membranes (Millipore, IPVH00010) by constant current 350 mA. After blocking with 3% BSA for 1 h at room temperature (RT), the PVDF membrane were immersed in the primary antibodies diluting solution at 4 °C overnight. Following removing primary antibodies, the secondary antibodies were added and incubated with PVDF membranes for 1 h at RT. The protein bands were detected by chemiluminescence solution. The antibodies are shown in Supplementary Table 2.

2.6. Immunofluorescence staining assay

NT2 cells and TCAM2 cells were cultured at 5×10^4 cells per well on coverslips in twelve-well plates. After 16–18 h, biotin labeled piR-36249 mimics and scrambled siRNA oligonucleotides (a control sequence with biotinylation) were transfected with INTERFERin® reagent. After transfection for 48 h, the cells were fixed with 4% freshly prepared paraformaldehyde (PFA) at RT for 15 min. The fixed cells were

permeabilized with 0.02% Triton X-100 for 5–10 min. Subsequently, cell slides were immersed in 3% BSA and blocked excess protein-binding sites. The cell samples were incubated with primary antibodies followed by secondary antibodies. The nucleus was stained with Hoechst 33342 solution. The immunostained cells were observed using a confocal microscope (OLYMPUS, FV1200).

2.7. Cell viability assay

CCK8 has been widely accepted as a representative cell viability indicator, which can produce formazan dye during cellular proliferation, and its yield is proportional to the number of cells. Cell viability was measured using a CCK-8 reagent (Vazyme, A311-01). Transfected cell samples were seeded for 96-well plates with 1000 cells per well. Then 10 μl CCK8 working solution were added to 90 μl culture medium in each group and incubated at 37 °C for 1–2 h in a cell incubator. The optical density (OD) value was detected for each well at a wavelength of 450 nm using a microplate reader.

2.8. Colony formation assay

After treatment, 1000 cells were incubated in each well of six-well plates with the suitable culture conditions. After incubation for 7–14 days, removed the medium and washed colonies twice with $1 \times$ PBS. Then, 4% freshly PFA was added to target cells and co-incubated at RT for 15 min. After fixation, cells were treated with 0.2% crystal violet (Meilun Biology, CAS No. 528-62-9) for 20 min at RT. Stained colonies were visualized under bright field microscopy.

2.9. 5-Ethynyl-2′-deoxyuridine (edu) assay

The EdU assay was carried out with a Beyoclick™ EdU-647 Cell Proliferation Assay Kit (Beyotime, C0081S). After treatment, the cells were immersed in EdU working solution and reaction for 2 h in a cell incubator. The EdU medium mixture was removed thoroughly, and 4% PFA in $1 \times$ PBS was used to fix the cells for 10–15 min at RT. The fixed cells were washed 3 times with 3% BSA for 5 min, and 0.02% Triton X-100 was added to target cell, permeabilized for 10 min at RT. Click reaction solution was then added to react for 30 min at RT in the dark. After washing 3 times with 3% BSA for 5 min, Hoechst 33342 was stained the cell nucleus for 2–3 min. The immunostained cells were imaged using a microscope (OLYMPUS, IX73), and quantitative analysis of cell images was performed by ImageJ software.

2.10. Wound healing/scratch assay

Cell migration and motor ability were assessed by wound healing/scratch assays according to previously reported [33]. After transfection treatment, TCAM2 and NT2 cells were seeded into twelve-well plates. The pipette tips were applied to make perpendicular scratches along the centerline of the cell culture plate, followed by washing with $1 \times$ PBS and incubating in DMEM with low concentration serum to culture the cells. The cells were then photographed and recorded with a microscope at 0 h or 24 h. The quantitative cell images were analyzed by ImageJ software.

2.11. Cell apoptosis assay

The cell apoptosis analysis was conducted according to the instructions of the apoptosis detection kit (Vazyme, A211-01). Briefly, cell pellets were collected after transfection and washed twice with precooled $1 \times$ PBS. Then, 100 μL fixation buffer was added to resuspend the cell pellets, Annexin V-FITC dye was applied to label apoptotic cells and PI solution was used for staining nucleus. The cells were incubated with two stain fluids at RT for 10 min in the dark. Subsequently, 400 μL fixation buffer was added to the cells. Samples are need to measure by

flow cytometry within 1 h and analyzed by FlowJo_V10_CL.

2.12. Biotinylated piRNA pull-down

Biotin-labeled-piRNA pull-down experiments were conducted as previously recorded [34]. Briefly, the 3′-end biotinylated piR-36249 mimics and negative control were transfected into NT2 cells. The cells were collected after transfection for 24 h and washed twice with $1 \times$ PBS. Then, 1 mL lysis buffer (0.3% NP-40, 100 mM KCl, 5 mM MgCl$_2$, 20 mM Tris-HCl pH 7.4) was added and applied to lyse cells. Meanwhile, RNase inhibitor and protease inhibitor cocktail were added to lysis buffer. After 65 min of incubation at 4 °C with rotation. The cell lysates were obtained by centrifuging at $14,000 \times g$ for 10 min. Then, magnetic beads (Invitrogen, 11205D) were added to each supernatant. After 2 h of incubation at 4 °C, the beads were isolated using 8% SDS–PAGE gels and Coomassie blue staining. Then, the sections were destained and analyzed by mass spectrometry (MS).

2.13. Dual-luciferase reporter assay

Our priority is to construct some recombinant plasmid, the wild-type *PTBP3*-3′UTR or *OAS2*-3′UTR sequence containing the putative piR-36249 target site or mutant *PTBP3*-3′UTR or *OAS2*-3′UTR sequence was cloned into the pmirGLO vector (Promega, E1330). Then, NT2 cells were cotransfected with negative control or piR-36249 mimics and pmirGLO vector containing wild-type or mutant *PTBP3*-3′UTR or *OAS2*-3′UTR. After 48 h, Firefly or Renilla luciferase activities were measured according to the dual-luciferase system kit (Promega, E2920) on a CLARIOstar Microplate reader (BMG LAkBTECH).

2.14. RNA-binding protein immunoprecipitation (RIP) assay

RNA-binding protein immunoprecipitation (RIP) assays in cells were conducted as previously recorded [32]. Briefly, the cells were seeded in 10–15 cm dishes. When the cell density was approximately 90%, the cells were washed twice with ice-cold $1 \times$ PBS (not digested). Then, cells crosslinked with 400 mJ UV were collected and removed as much $1 \times$ PBS as possible with a pipette tip carefully. The cell sample was suspended in NET-N buffer for 1–2 h at 4 °C under rotating conditions. The cell lysate was sonicated for 4 min in an ice bath with 4 s on and 6 s off pulse intervals. The lysates were spun at $16,000 \times g$ for 10 min at 4 °C. Then, specific antibodies or isotype IgG were added to the supernatant and incubated overnight at 4 °C. Protein A/G Magnetic Beads (Thermo, 88803) were added to each sample followed by incubation for 2 h at 4 °C. Finally, the beads were washed and collected for RT-qPCR analysis.

2.15. RNA sequencing and analysis

After treatment, three independent RNA samples in each group (piR-36249 mimics or negative control) were prepared as described above. RNA library preparation and sequencing were performed by Berry Genomics (Beijing). Then, we use FastQC (version 0.11.8) to do some quality control checks. Clean reads were mapped using HISAT2 (version 2.1.0) [35] to the GRCM38 Ensembl genome. The SAM files were sorted and converted to BAM files using SAMtools (version 1.7) [36]. The mapped reads were then counted using feature Counts (version 2.0.1) [37]. DEGs were determined using R package DESeq2 (version 1.26.0) [38] with a P-value <0.05 and an absolute value of log2FC > 1. Volcano map and heatmap generation were conducted, respectively, using R packages "ggplot2" (version 3.3.2) and "pheatmap" [Kolde R, Kolde MR. Package "pheatmap"2] (version 1.0.12 https://CRAN.R-project.org/package=pheatmap).

2.16. Statistical analysis

All statistical analyses were conducted using GraphPad software. To

assess the statistical significance of a difference between two treatments, we used unpaired, two-tailed Student's t tests. Data are shown as the mean ± SEM, and statistical significance is set as *P < 0.05, **P < 0.01, and ***P < 0.001.

3. Results

3.1. piR-36249 is downregulated in testicular cancer

To study the role and mechanism of PIWI-interacting RNAs (piRNAs) in testicular cancer, we collected human testicular cancer tissues and subsequently validated the differential expression of piR-36249 by RT-qPCR. We found that piR-36249 showed a significantly decreasing trend in testicular cancer tissue compared to the control (Fig. 1A). Multiple alignment analysis of the piR-36249 *(DQ598183)* locus according to the UCSC database showed that it is conserved among mice, rhesus monkeys and humans (Fig. 1B). In addition, we also validated the level changes of piR-36249 in normal testicular Leydig cells TM3, normal spermatogonial cells GC1, testicular nonspermatogonial carcinoma cells NT2, and testicular spermatogonial carcinoma cells TCAM2. The results showed that piR-36249 had low expression in testicular cancer cells compared with normal testicular cells (Fig. 1C and D). The results suggested that the conserved piR-36249 may function in inhibiting testicular cancer development.

3.2. piR-36249 is distributed in the cytoplasm of NT2 and TCAM2 cells

piRNAs may be distributed in the nucleus or cytoplasm or both and play multiple roles in different subcellular localizations to perform different functions. Considering that the regulatory mechanism of piRNAs is related to their situations, we dissected target cells into the nucleus and cytoplasm to characterize the subcellular localization of piR-36249 in human nonspermatogonial carcinoma cells (NT2) and

human seminoma cells (TCAM2). The cellular distribution analysis suggested that GAPDH protein was only enriched in the cytoplasm; whereas LaminB1 was mainly distributed in the nucleus, validating the accuracy of our fractionation (Fig. 2A). We subsequently validated the expression of piR-36249 in differential components from NT2 and TCAM2 cells by RT-qPCR, showing that piR-36249 was mainly expressed in the cytoplasm, with only a tiny portion in the nucleus (Fig. 2B and C). We also performed immunofluorescence (IF) to confirm the subcellular localization of transfected biotin-labeled piR-36249 mimics. The IF analyses agreed with the RT-qPCR results, and piR-36249 was largely located in the cytoplasm of testicular cancer cells (Fig. 2D and E). Together, these results suggest that cytoplasmic piR-36249 may participate in testicular cancer cell progression.

3.3. piR-36249 suppresses the malignant phenotype of NT2 and TCAM2 cells

To study whether piR-36249 functions in testicular cancer cells, we performed overexpression and knockdown experiments using piR-36249 mimics and inhibitor, respectively. By RT-qPCR analysis, we confirmed that transfection was effective in NT2 and TCAM2 cells (Fig. 3A and B). The CCK8 assays revealed that piR-36249 significantly suppressed NT2 and TCAM2 cell proliferation, whereas inhibition of piR-36249 promoted cell proliferation (Fig. 3C–F). We also performed an EdU (5-ethynyl-2′-deoxyuridine) assay in NT2 and TCAM2 cells to examine cell proliferation, and similar phenotype were again determinated in NT2 and TCAM2 cells (Figs. S1A–D). Furthermore, colony formation analysis showed that the tumor formation and colony formation ability of NT2 and TCAM2 cells were also inhibited upon piR-36249 overexpression (Fig. 3G–J). It is known that the cell scratch assay can serve as a way to assess cell invasion. We next performed wound healing analysis to investigate cell invasion and repair ability. This result was consistent with the fact that piR-36249 can suppress the
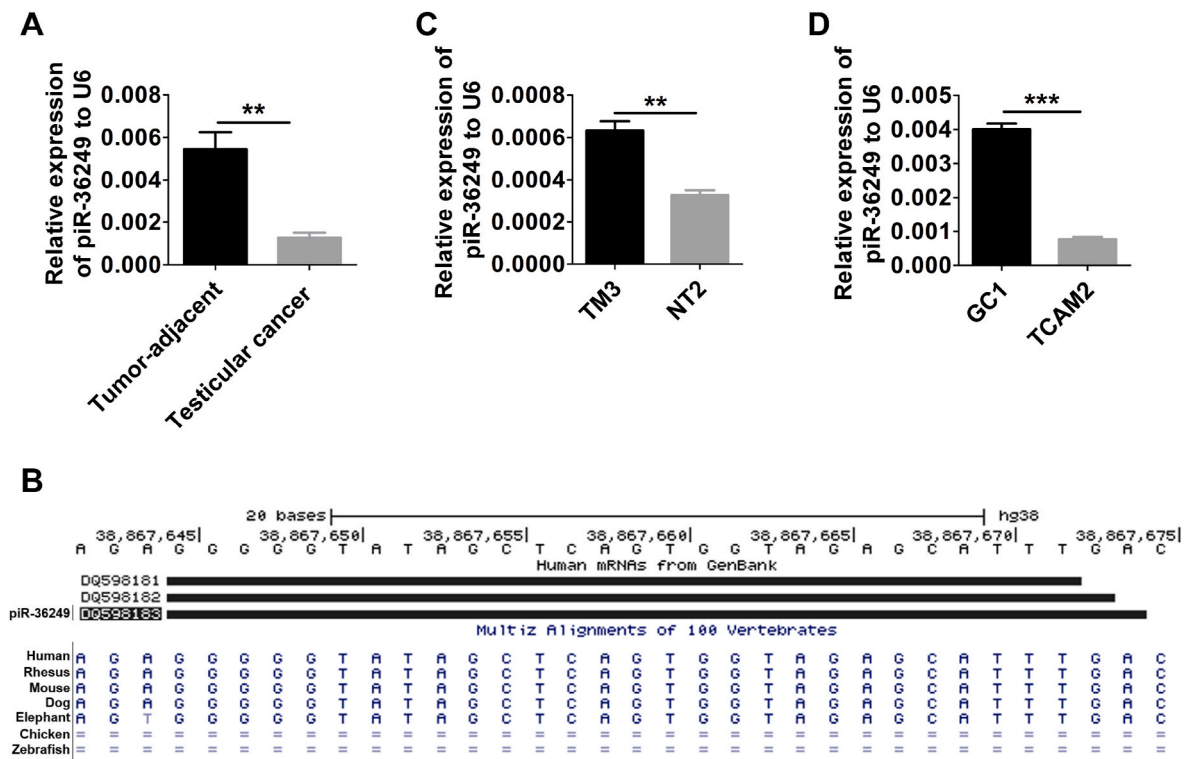

Fig. 1. piR-36249 is downregulated in testicular cancer. (A) Relative expression levels of piR-36249 in human testicular cancer and tumor-adjacent tissue were detected by RT-qPCR (n = 3). (B) The piR-36249 gene *(DQ598183)* information shown in the UCSC human database. (C–D) Relative expression levels of piR-36249 in different normal germ cells and cancer cells were detected by RT-qPCR (n = 3). Normal nonspermatogonial cell line (TM3), nonspermatogonial carcinoma cell line (NT2), normal spermatogonial cell line (GC1) and testicular spermatogonial carcinoma cell line (TCAM2).
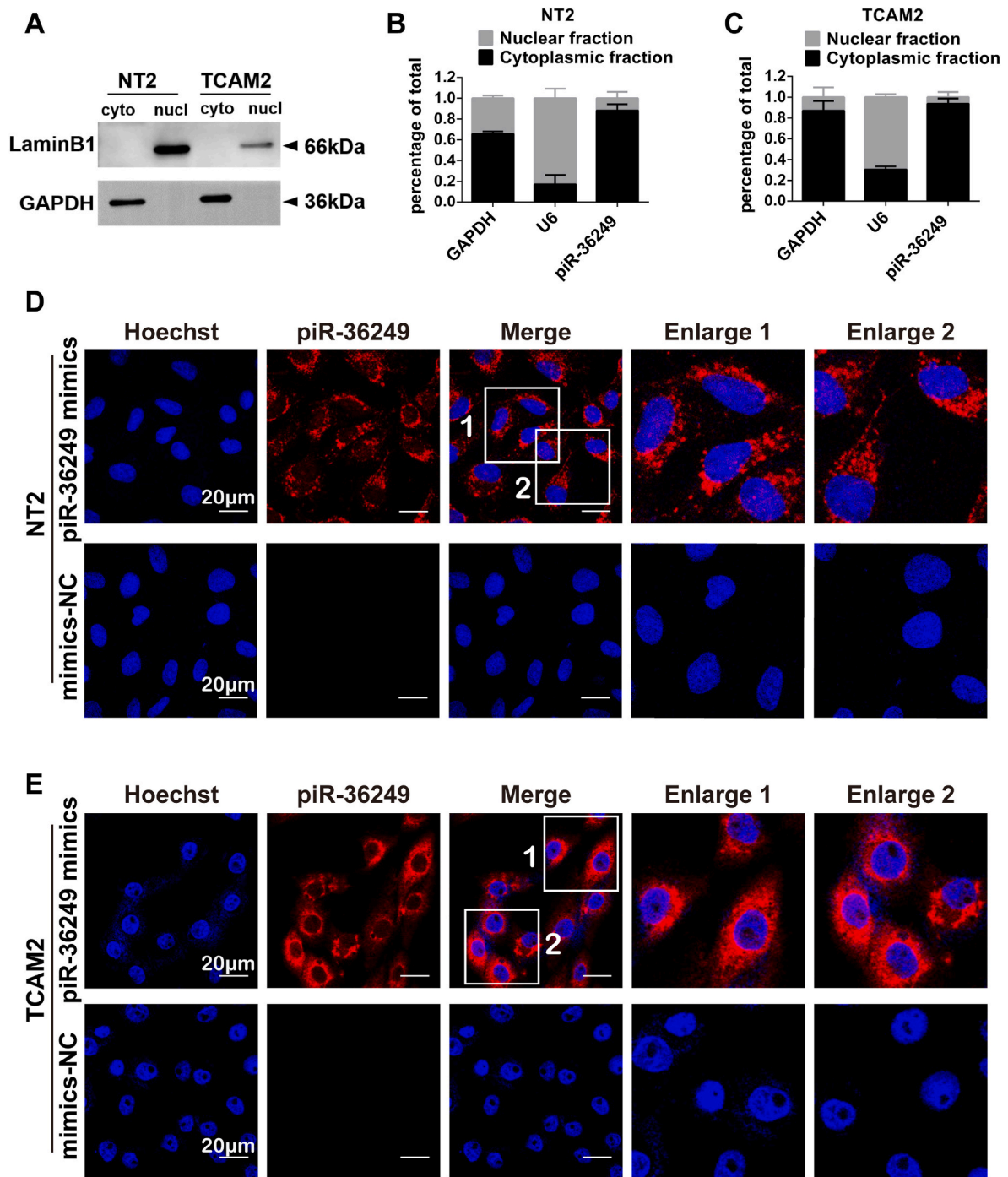
Fig. 2. piR-36249 is distributed in the cytoplasm of NT2 and TCAM2 cells. (A) The fractions of cytoplasmic and nuclear in NT2 and TCAM2 cells was identified by western blot. GAPDH is regarded as a cytoplasmic marker, as well as Lamin B1 is a nuclear marker. (B–C) Distribution of piR-36249 in the cytoplasm and nucleus of NT2 and TCAM2 cells, respectively (n = 3). (D–E) Subcellular localization of exogenous piR-36249 in NT2 and TCAM2 cells transfected with biotin-labeled piR-36249 mimics or negative control (mimics NC) by confocal microscopy. piR-36249 was then stained with antibiotin555 (red), and cell nuclei were stained by using Hoechst 33342 (blue). Scale bars, 20 μm.

migration ability of NT2 and TCAM2 cells, while knockdown of piR-36249 increases viability (Fig. 3K-N). These data indicated that piR-36249 inhibits the malignant phenotypes of testicular cancer cells, including proliferation, colony formation, and migration.

3.4. piR-36249 promotes apoptosis and upregulates proapoptotic related proteins

To investigate whether piR-36249 suppresses cell viability in testicular cancer cells by enhancing cell apoptosis, we then recorded the number of apoptosis-positive cells after NT2 and TACM2 cells were transfected with piR-36249 mimics or inhibitor by flow cytometry (Fig. 4A and B). The analysis data showed that following overexpression of piR-36249, the number of apoptotic-positive cells is significantly increased in NT2 cells, while the piR-36249 inhibitor did not have a dramatic effect on apoptosis progression (Fig. 4C). Furthermore, piR-36249 upregulation or inhibition had no obvious interference with cell apoptosis in TCAM2 cells (Fig. 4D).
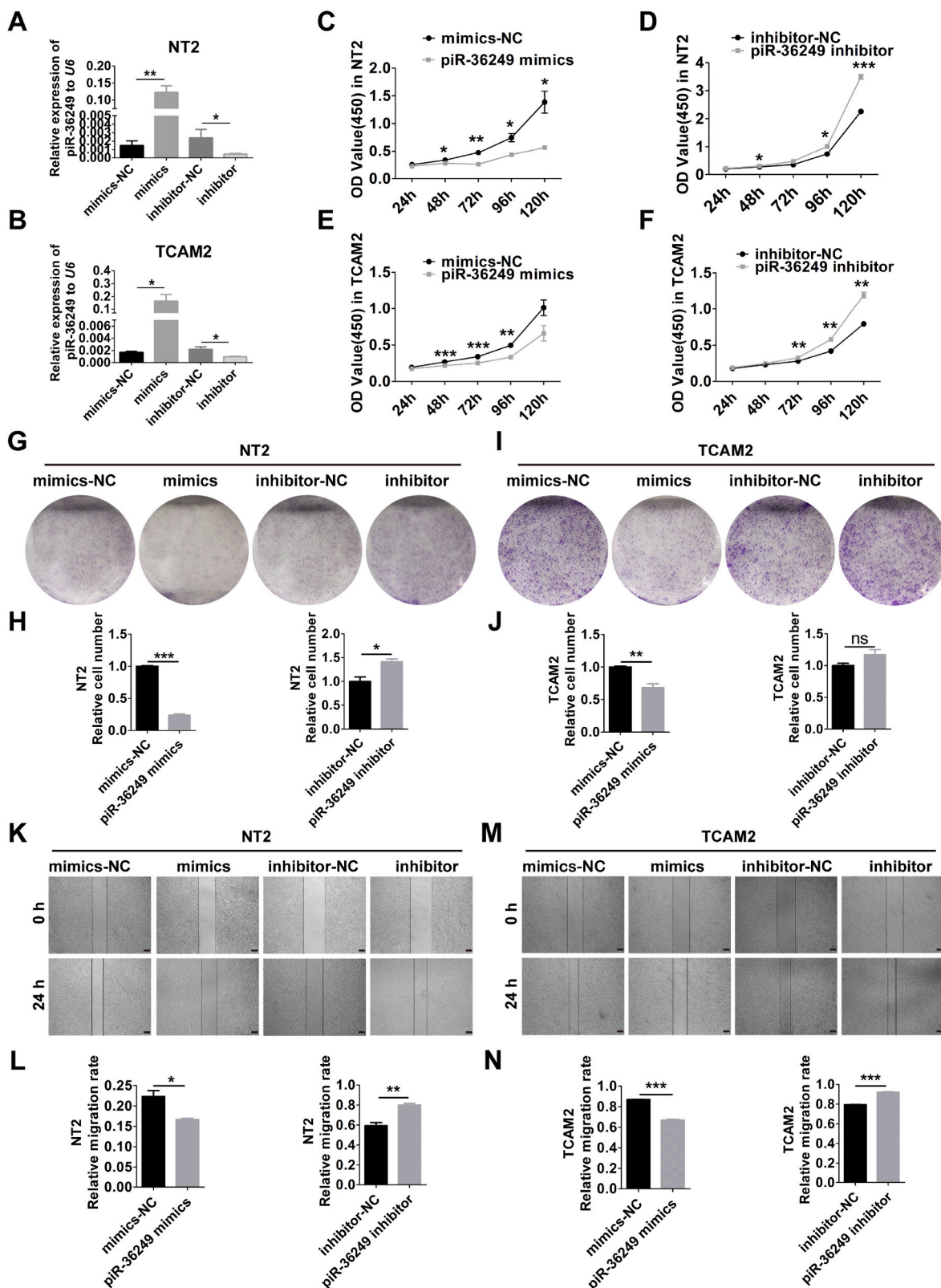
Fig. 3. piR-36249 suppresses testicular cancer cell proliferation, colony formation and cell migration ability. (A–B) Relative expression levels of piR-36249 after in vitro transfection of piR-36249 mimics or inhibitor in NT2 and TCAM2 cells were quantified by RT-qPCR (n = 3). (C–F) Effect of piR-36249 mimics or inhibitor on NT2 and TCAM2 cell proliferation determined by CCK8 assay (n = 3). (G and I) Effect of piR-36249 mimics or inhibitor on the colony formation ability of testicular cancer cells. (H and J) Quantification of colony forming ability relative to the control (n = 3). (K–N) The cell migration ability of NT2 and TCAM2 cells was analyzed and quantification of the effect of piR-36249 overexpression or inhibition on NT2 (K–L) and TCAM2 (M − N) cell migration ability. Scale bar: 200 μm.
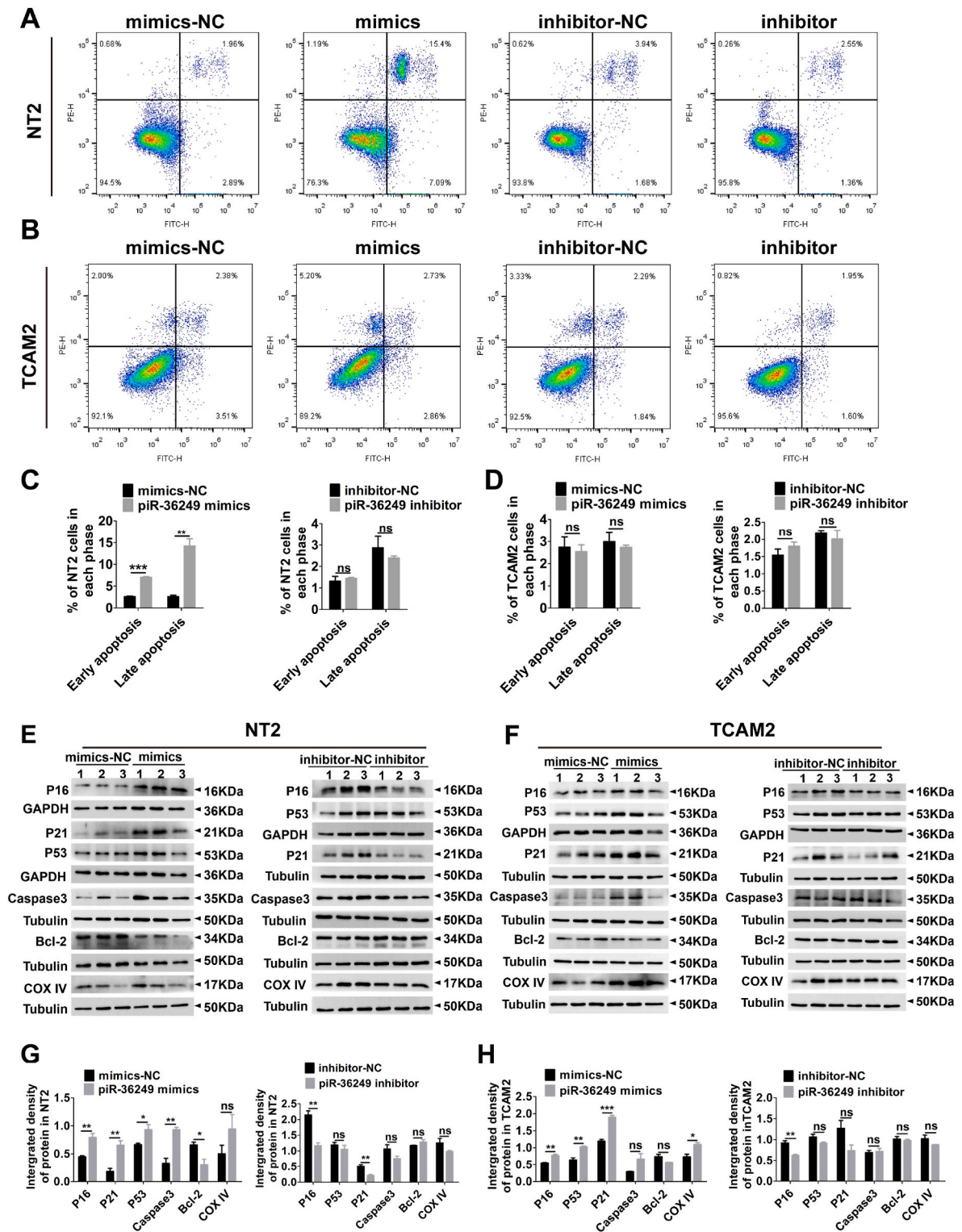
Fig. 4. piR-36249 promotes apoptosis and upregulates proapoptotic related proteins. (A–B) Effect of piR-36249 on apoptosis by flow cytometry analysis in NT2 cells and TCAM2 cells. (C–D) The number of positive apoptotic cells was quantified in NT2 cells and TCAM2 cells by FlowJo_V10_CL (n = 3). (E–F) The protein levels of p16, p53, p21 and expression level of protein COX IV, caspase 3, Bcl-2 were measured by western blot assay after overexpression or inhibition of piR-36249 in NT2 and TCAM2 cells. (G–H) Quantification of western blots for cell cycle modulators (p21, p53 and p16) and apoptosis-related proteins (caspases 3, COX IV and Bcl-2), n = 3.

On the other hand, we carried out western blot assay and measured the protein levels of the p53 and p21 genes, which are two important regulators in cell cycle, cell survival and participated in protection against tumorigenesis [39,40]. We also detected the p16 protein

expression level, which has been regarded as negatively regulator in mostly cancers [41]. In addition, we tested the expression levels of other proteins involved in the apoptotic signaling pathway, such as the proapoptotic-related proteins caspase 3 and COX IV (cytochrome *c*

oxidase subunit IV) and the antiapoptotic protein Bcl-2 [42,43]. We found a significant increasing trend of p16, p21, p53, caspase 3 and COX IV proteins upon overexpression of piR-36249 in NT2 and TCAM2 cells (Fig. 4E–H). We also found that piR-36249 can effectively block the function of the protein Bcl-2 in NT2 and TCAM2 cells. However,

inhibition of piR-36249 did not completely reverse the expression of these proteins (Fig. 4E–H). These results indicated that piR-36249 affects testicular cancer cell proliferation by activating proapoptotic proteins and promoting cell apoptosis.
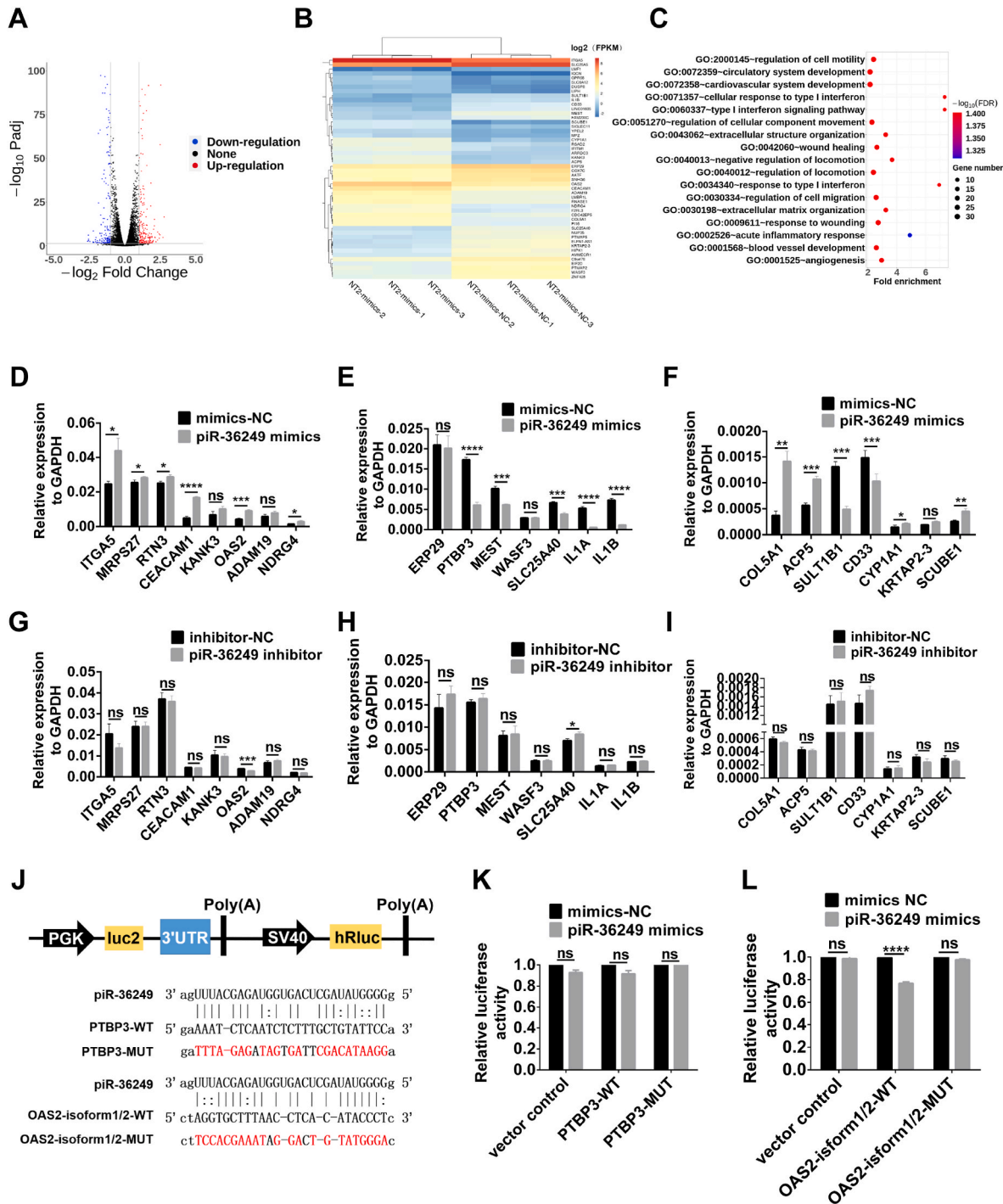

Fig. 5. piR-36249 binds to the 3′UTR of 2′-5′-oligoadenylate synthetase 2 (*OAS2*) mRNA and upregulates OAS2 expression. (A) Volcano plots showing the expression profiles of differentially expressed genes (DEGs) upon overexpression of piR-36249 (mimics) in NT2 cells. Black dots mean no change, red dots represent upregulated trend, blue dots are downregulated. (B) The heatmap shows the fold changes of the top 50 differentially expressed genes with base mean 100 in NT2 cells transfected with piR-36249 mimics and mimics-negative control. (C) Gene ontology enrichment of DEGs in NT2 cells. (D–F) The expression level of 22 candidate DEGs in NT2 cells after transfection of piR-36249 mimics and NC was detected by RT–qPCR, using *GAPDH* mRNA as an internal control (n = 3). (G–I) RT-qPCR analysis was applied to detect the same genes as above in NT2 cells transfected with piR-36249 inhibitor and NC (n = 3). (J) Schematic diagram of the potential binding sites of piR-36249 on *PTBP3* and *OAS2* mRNA. (K–L) Relative luciferase activity of *PTBP3*-3′UTR and *OAS2*-3′UTR recombinant plasmids was measured upon cotransfection of piR-36249 mimics or mimics NC in NT2 cells (n = 3).

3.5. piR-36249 binds to the 3′UTR of 2′-5′-oligoadenylate synthetase 2 (OAS2) mRNA and upregulates OAS2 expression in NT2 cells

Recent evidence suggests that piRNAs can also bind to mRNA through incomplete base pairing to suppress or activate gene expression. To identify the potential targets of piR-36249, we performed a transfection assay in NT2 cells with piR-36249 mimics or negative control (NC). Then, we collected three independent RNA samples in each group and subjected them to RNA sequencing (mRNA-Seq; Data number GSE213411). We identified 401 differentially expressed genes (DEGs) among different samples with a P value < 0.05 and fold change >2. Of these, 219 genes were significantly upregulated, and the rest were downregulated in NT2 cells upon piR-36249 overexpression (Fig. 5A). The top 50 DEGs were depicted in the heatmap obtained via hierarchical clustering analysis (Fig. 5B). The GO (gene ontology) enrichment analysis showed that many differentially expressed protein coding genes were associated with some biological processes, such as wound healing and tumor immune responses (Fig. 5C).

We subsequently validated the differential expression of candidate DEGs by RT-qPCR, showing that 17 out of 22 genes were statistically significantly differentially expressed after piR-36249 overexpression (Fig. 5D–F). However, when endogenous piR-36249 was suppressed by the inhibitor, the expression of these genes was not statistically significantly compensated (Fig. 5G–I). We further used miRanda software (miRanda: http://www.bioinformatics.com.cn) to select and identify the target genes of piR-36249 among the 17 confirmed DEGs. Among the potential target genes, we found that piR-36249 might interact with the 3′UTRs of *PTBP3* and *OAS2* mRNAs, which were downregulated or upregulated, respectively, by piR-36249 mimics. We then cloned the 3′UTRs of these two genes into dual-luciferase reporter plasmids (Fig. 5J) and verified the site of interaction between piR-36249 and *PTBP3* or *OAS2* mRNA. The results revealed that the luciferase activity was not affected for the *PTBP3* 3′UTR (Fig. 5K). It was significantly reduced in NT2 cells cotransfected with piR-36249 mimics and wild-type (WT) *OAS2*-isoform1/2–3′UTR luciferase reporter gene plasmids, which was abolished when the *OAS2*-isoform1/2–3′UTR was mutated (MUT) (Fig. 5L). These results demonstrated that piR-36249 targets the 3′UTR of *OAS2*-isoform 1/2 mRNA.

We further determined the effects of piR-36249 on *OAS2* expression by detecting OAS2 protein levels in response to piR-36249 mimics or inhibitors in transfected NT2 cells. Our data showed that piR-36249 mimics increased and the inhibitor decreased the OAS2 protein levels in NT2 cells (Fig. 6A and B), consistent with the above results that *OAS2* mRNAs were upregulated by piR-36249 mimics. Next, to verify whether knockdown of *OAS2* would produce the same cell phenotype of inhibiting cell proliferation as piR-36249, we designed two siRNAs specifically targeting *OAS2* isoform 1 and isoform 2 and transfected them into NT2 cells to knockdown *OAS2*. Western blot analysis showed that the protein level of *OAS2* was significantly reduced upon siRNA transfection (Figs. S2A–B). Then, EdU assays and scratch wound healing assays were carried out, and the data showed that NT2 cell proliferation and invasion ability were inversely proportional to the expression levels of *OAS2* (Figs. S2C–D and E-F), similar to what we observed after knockdown of piR-36249. We thus speculated that piR-36249 restrains testicular cancer cell progression by upregulating *OAS2* expression.

3.6. piR-36249 and DHX36 together inhibit testicular cancer cell progression by upregulating OAS2

As cytoplasmic piRNAs can interact with certain proteins to perform their function, we conducted an RNA pull-down assay (using biotin-conjugated piR-36249 oligonucleotides as the bait) combined with mass spectrometry (MS) analysis in NT2 cells to identify potential piR-36249-associated proteins (Fig. S3A). The results showed that piR-36249 might interact with some proteins involved in cell metabolic processes and RNA splicing (Fig. 6C). Intriguingly, they can also affect

mRNA transcription and translation. Further validating pulled down proteins through Western blot, we found that piR-36249 bound to ATP-dependent DNA/RNA helicase DHX36 (DHX36) (Fig. 6D).

Additional analysis of DHX36 expression levels in human testicular cancer and nontumor counterparts by using GEPIA2 databases (Gene Expression Profiling Interactive Analysis, GEPIA 2 (http://gepia2. cancer-pku.cn/#index)) showed that DHX36 was significantly reduced in TGCT (Fig. S3B). A study reported that DHX36 can directly target the 3′UTR and 5′UTR of mRNAs to activate translation [44]. Given the interaction between piR-36249 and *OAS2* mRNA, we wanted to predict the interaction probability between DHX36 protein and *OAS2* mRNA by a predictive database (RNA-Protein Interaction Prediction, RPISeq, http ://pridb.gdcb.iastate.edu/RPISeq/). Our data showed that the DHX36 protein was likely to aim to the 3′UTR of *OAS2* mRNA (Fig. S3C). We next carried out a RIP (RNA immunoprecipitation) assay with DHX36 antibodies and confirmed the interaction between the helicase DHX36 and *OAS2* mRNA (Fig. 6E and F). To determine the underlying molecular mechanism of how DHX36 intercedes *OAS2* mRNA expression, we first detected the expression level of *OAS2* following transfection with DHX36 siRNA in the NT2 cell line (Fig. 6G and H). The results showed that the protein level of *OAS2* was decreased but that of mRNA was increased upon DHX36 knockdown (Fig. 6I–K), indicating that DHX36 knockdown inhibits the protein expression level of *OAS2* and increases its mRNA abundance, which potentially suggests a translation-promoting effect of DHX36 on *OAS2* mRNA. These data suggest that piR-36249 and DHX36 together inhibit testicular cancer cell progression by upregulating OAS2 protein levels.

4. Discussion

piRNAs have been reported to be abundantly enriched in the reproductive system and closely related to spermatogenesis and germ cell development, as well as associated with reproductive diseases and developmental disorders in a variety of species. Recent studies have shown that piRNAs are also expressed in somatic tissues and that abnormal expression is closely associated with the development of some human cancers [45,46]. For example, piR-54265 interacts with PIWIL2 protein to promote the progression of colorectal cancer [47]. In addition, piRNAs can function independently of PIWI proteins in cancer systems. For example, piRNA-30473 can promote tumorigenesis by enhancing the expression of WTAP (a methylase) and upregulating HK2 (hexokinase 2) m6A levels in B cell lymphoma [48]. Nevertheless, the underlying mechanism of how piRNAs function in the survival of human testicular cancer is still unknown.

In the present work, we have demonstrated that piR-36249 binds to the 3′UTR of 2′-5′-oligoadenylate synthetase 2 (*OAS2*) mRNA and upregulates OAS2 protein expression in a PIWI-independent manner. Several studies have identified that *OAS2* serves as a regulator and contributes to the regulation of important physiological processes including cell proliferation, cell differentiation and cell apoptosis [49–51]. Importantly, it has been shown that *OAS2* is a valid suppressor and plays an important role in modulating the occurrence and progression of some tumors. In colorectal cancer, *OAS2* inhibits invasion and metastasis by upregulating E-cadherin, claudin-1 and β-catenin [52]. Furthermore, they demonstrated that vascular endothelial growth factor D (VEGFD) is upregulated in *OAS2*-inhibiting cells, which is required for the dissemination of colorectal cancer [52]. Another study reported that *OAS2* effectively inhibited cell proliferation in pancreatic β-cells [53]. High mRNA expression of *OAS2* is also correlated with favorable prognosis for all breast cancer patients tested [51]. Recently, it has been reported that *OAS2,* as an interferon IFN-stimulated gene, is repressed in mesenchymal/cancer stem cells [54], while the interferon response is related to the survival and metastatic activity of breast cancers [55].

In our study, *OAS2* knockdown cells consistently showed increased proliferation and invasion compared to the control cells. piR-36249 can
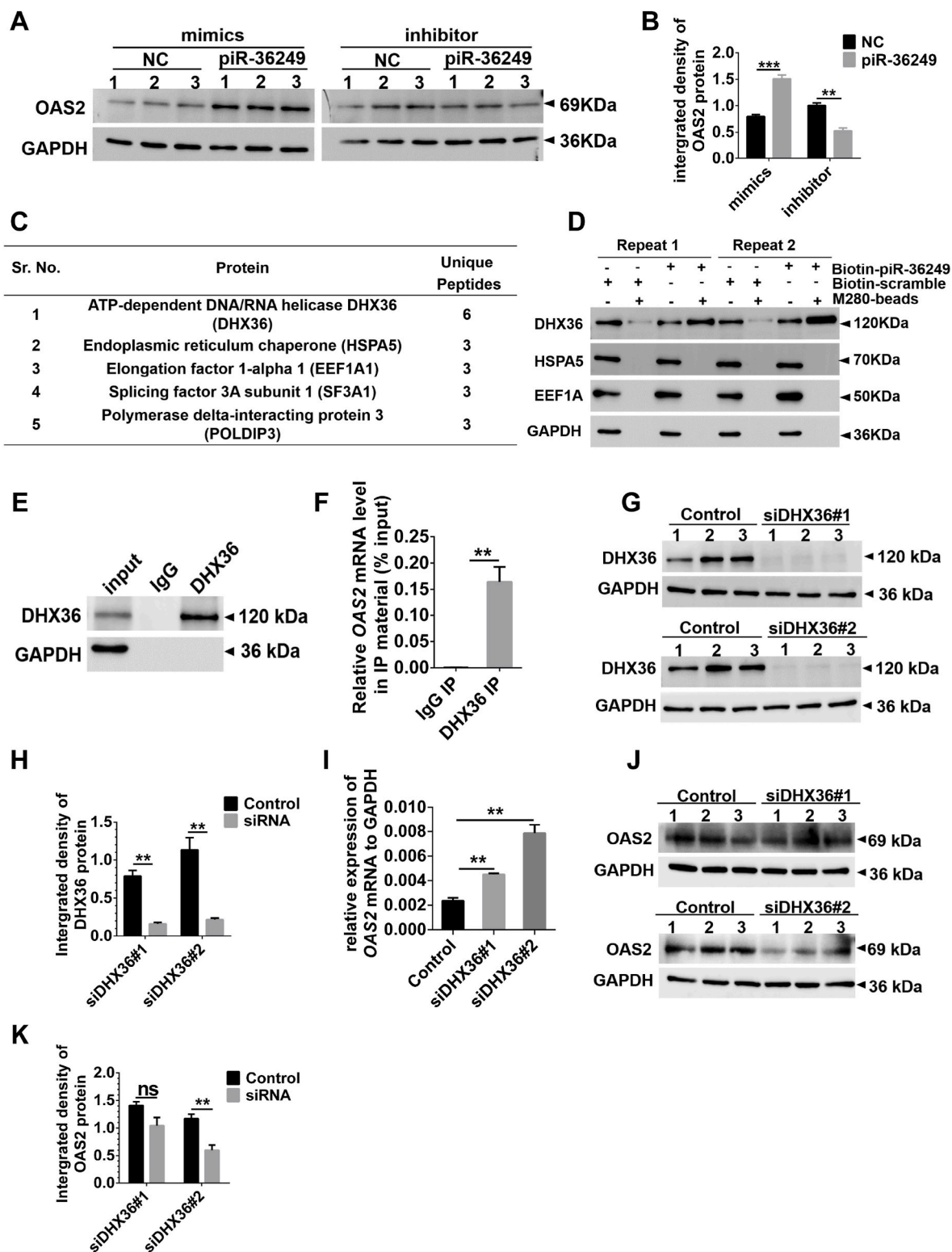
Fig. 6. piR-36249 and DHX36 together inhibit testicular cancer cell progression by upregulating OAS2. (A–B) Representative images and quantification of Western blots for OAS2 protein upon transfecting piR-36249 mimics and inhibitor in NT2 cells (n = 3). (C) List of top piR-36249 binding protein candidates detected in NT2 cells by RNA pull down–mass spectrometry. (D) Western blots assessed the specific association of piR-36249 with DHX36 in pull-down lysates of two repeated experiments. (E) Western blots assessed DHX36 immunoprecipitation by anti-DHX36 antibody in the NT2 cell line (n = 3). (F) Relative enrichment of *OAS2* binding to DHX36 in IP was detected by RT–qPCR assay (n = 3). (G–H) Representative image and quantification of Western blot for DHX36 protein following in vitro transfection of siRNAs in NT2 cells (n = 3). (I) The expression level of *OAS2* mRNA after DHX36 knockdown in the NT2 cell line was measured by RT-qPCR analysis (n = 3). (J–K) Western blot assay and quantification of OAS2 protein in the NT2 cell line following DHX36 knockdown (n = 3).

promote *OAS2* mRNA expression, and inhibition of piR-36249 increases the malignant phenotype of testicular cancer cells. Furthermore, our RNA-seq data showed that piR-36249 overexpression downregulates wound healing and the blood vessel development pathway. All of these data support that piR-36249 inhibits testicular cancer cell survival and migration by activating the expression of *OAS2*. However, more in-depth research and in nude mouse models are necessary to disclose the detailed effect of piR-36249 and *OAS2* on in testicular cancer cell growth and migration.

Interestingly, studies have shown that piRNAs can directly bind to 3′UTRs of mRNAs and recruit *cis*-acting AU-rich elements to form the MIWI/piRNA/eIF3f/HuR supercomplex to activate translation during mouse spermatogenesis [56]. We thus speculated that piR-36249 might interact with some proteins to activate *OAS2* gene expression. Our piRNA pull-down-MS data showed that piR-36249 interacts with the ATP-dependent DNA/RNA helicase DHX36, and RIP assay showed that DHX36 interacts with *OAS2* mRNA. In addition, the protein level of *OAS2* was decreased but that of mRNA was increased upon DHX36 knockdown. This result is consistent with a recent report showing that DHX36 knockout results in a significant increase in target mRNA abundance [44]. It is also an interesting phenotype indicating a divergent function of DHX36 in regulating *OAS2* at the mRNA and protein levels. For mRNA regulating function, DHX36 was first defined as an ARE (AU-rich element, ARE)-bound RBP (RNA-binding protein) that regulates post-transcriptional processing and RNA decay [57,58]. Thus, the increased *OAS2* mRNA we observed upon DHX36 knockdown might be due to the loss of RNA decay or mRNA instability function of DHX36. However, we didn't find any typical decay factors involved in mRNA degradation in piR-36249 pull-down mass spectrometry (MS) samples (Supplemental Table S3).

For protein level regulation, it has been shown that the binding of DHX36 in mRNA 3′UTR and 5′UTR results in increased translational efficiency of target mRNA in a helicase activity-dependent manner [44, 59,60]. The decreased OAS2 protein level we observed upon DHX36 knockdown thus indicated that DHX36, which binds to *OSA2* mRNA, might function in promoting *OAS2* mRNA translation whose knockdown decreased translation efficiency and decreased the protein level of *OAS2*. Additionally, the increased mRNA level and decreased protein level of *OAS2* in DHX36 knockdown also imply that the completion of a translation cycle of *OAS2* might trigger its mRNA degradation and/or reflects a feedback result from the retarded translation. On the other hand, GO enrichment pathway analysis of piR-36249 pull-down MS results revealed that many potential piR-36249-associated proteins were associated with RNA splicing and mRNA metabolic pathways (Fig. S4A), which could also regulate the *OAS2* mRNAs amount and stability. Further detailed mechanism studies in the future will help to uncover how DHX36 knockdown affect *OAS2* expression at both RNA and protein levels. This will provide useful insights and implications revealing the multifunctionality of DHX36 as a single molecule.

Notably, DHX36 functions as a tumor suppressor to regulate tumor development at the posttranscriptional level. For example, DHX36 inhibits breast cancer growth by regulating the activities of cyclin-dependent kinases [61]. In non-small cell lung cancer (NSCLC), DHX36 can also serve as a tumor suppressor and potentially become a new target for anticancer therapy based on helicase-specific targeting [62]. We now provide evidence that DHX36 is downregulated in testicular cancer (from GEPIA2 databases) and, together with piR-36249, promotes OAS2 protein levels.

5. Conclusion

In this study, we found that piR-36249 interacts with the DHX36 protein and that piR-36249 targets *OAS2* mRNA on its 3′UTR through imperfect base-pairing interactions, which leads to the upregulation of the OAS2 protein. In turn, the upregulation of *OAS2* increases the cell inflammatory response, resulting in the suppression of malignant

phenotypes, including proliferation, colony formation ability, and migration. These data support that piRNA-36249 is a novel therapeutic target of testicular cancer and all results open up new directions for male infertility and testicular cancer research.

Data availability statement

The data supporting the findings of this study are available within the article and its supplemental materials. RNA sequencing data files has been deposited in the NCBI Gene Expression Omnibus (GEO) under accession number GSE213411, which is publicly accessible at https://www.ncbi.nlm.nih.gov/geo/.

Declaration of competing interest

The authors declare that they have no known competing financial interests or personal relationships that could have appeared to influence the work reported in this paper.

Appendix A. Supplementary data

Supplementary data to this article can be found online at https://doi.org/10.1016/j.ncrna.2022.12.004.

References

[1] A. Aravin, D. Gaidatzis, S. Pfeffer, M. Lagos-Quintana, P. Landgraf, N. Iovino, P. Morris, M.J. Brownstein, S. Kuramochi-Miyagawa, T. Nakano, M. Chien, J. J. Russo, J. Ju, R. Sheridan, C. Sander, M. Zavolan, T. Tuschl, A novel class of small RNAs bind to MILI protein in mouse testes, Nature 442 (2006) 203–207.

[2] Y. Xiao, A. Ke, PIWI takes a giant step, Cell 167 (2016) 310–312.

[3] R. Suzuki, S. Honda, Y. Kirino, PIWI expression and function in cancer, Front. Genet. 3 (2012) 204.

[4] R.J. Ross, M.M. Weiner, H. Lin, PIWI proteins and PIWI-interacting RNAs in the soma, Nature 505 (2014) 353–359.

[5] K.W. Ng, C. Anderson, E.A. Marshall, B.C. Minatel, K.S. Enfield, H.L. Saprunoff, W. L. Lam, V.D. Martinez, Piwi-interacting RNAs in cancer: emerging functions and clinical utility, Mol. Cancer 15 (2016) 5.

[6] L.T. Gou, P. Dai, J.H. Yang, Y. Xue, Y.P. Hu, Y. Zhou, J.Y. Kang, X. Wang, H. Li, M. M. Hua, S. Zhao, S.D. Hu, L.G. Wu, H.J. Shi, Y. Li, X.D. Fu, L.H. Qu, E.D. Wang, M. F. Liu, Pachytene piRNAs instruct massive mRNA elimination during late spermiogenesis, Cell Res. 25 (2015) 266.

[7] J.F. Su, A. Concilla, D.Z. Zhang, F. Zhao, F.F. Shen, H. Zhang, F.Y. Zhou, PIWI-interacting RNAs: mitochondria-based biogenesis and functions in cancer, Genes Dis. 8 (2021) 603–622.

[8] J. Cheng, J.M. Guo, B.X. Xiao, Y. Miao, Z. Jiang, H. Zhou, Q.N. Li, piRNA, the new non-coding RNA, is aberrantly expressed in human cancer cells, Clin. Chim. Acta 412 (2011) 1621–1625.

[9] L. Tan, D. Mai, B. Zhang, X. Jiang, J. Zhang, R. Bai, Y. Ye, M. Li, L. Pan, J. Su, Y. Zheng, Z. Liu, Z. Zuo, Q. Zhao, X. Li, X. Huang, J. Yang, W. Tan, J. Zheng, D. Lin, PIWI-interacting RNA-36712 restrains breast cancer progression and chemoresistance by interaction with SEPW1 pseudogene SEPW1P RNA, Mol. Cancer 18 (2019) 9.

[10] A. Fu, D.I. Jacobs, A.E. Hoffman, T. Zheng, Y. Zhu, PIWI-interacting RNA 021285 is involved in breast tumorigenesis possibly by remodeling the cancer epigenome, Carcinogenesis 36 (2015) 1094–1102.

[11] C. Zhao, Y. Tolkach, D. Schmidt, M. Toma, M.H. Muders, G. Kristiansen, S. C. Muller, J. Ellinger, Mitochondrial PIWI-interacting RNAs are novel biomarkers for clear cell renal cell carcinoma, World J. Urol. 37 (2019) 1639–1647.

[12] Y. Li, X. Wu, H. Gao, J.M. Jin, A.X. Li, Y.S. Kim, S.K. Pal, R.A. Nelson, C.M. Lau, C. Guo, B. Mu, J. Wang, F. Wang, J. Wang, Y. Zhao, W. Chen, J.J. Rossi, L.M. Weiss, H. Wu, Piwi-interacting RNAs (piRNAs) are dysregulated in renal cell carcinoma and associated with tumor metastasis and cancer-specific survival, Mol. Med. 21 (2015) 381–388.

[13] D. Mai, Y. Zheng, H. Guo, P. Ding, R. Bai, M. Li, Y. Ye, J. Zhang, X. Huang, D. Liu, Q. Sui, L. Pan, J. Su, J. Deng, G. Wu, R. Li, S. Deng, Y. Bai, Y. Zhang, W. Tan, C. Wu, T. Wu, J. Zheng, D. Lin, Serum piRNA-54265 is a New Biomarker for early detection and clinical surveillance of Human Colorectal Cancer, Theranostics 10 (2020) 8468–8478.

[14] J. Yin, X.Y. Jiang, W. Qi, C.G. Ji, X.L. Xie, D.X. Zhang, Z.J. Cui, C.K. Wang, Y. Bai, J. Wang, H.Q. Jiang, piR-823 contributes to colorectal tumorigenesis by enhancing the transcriptional activity of HSF1, Cancer Sci. 108 (2017) 1746–1756.

[15] J. Yin, W. Qi, C.G. Ji, D.X. Zhang, X.L. Xie, Q. Ding, X.Y. Jiang, J. Han, H.Q. Jiang, Small RNA sequencing revealed aberrant piRNA expression profiles in colorectal cancer, Oncol. Rep. 42 (2019) 263–272.

[16] S.J. Zhang, J. Yao, B.Z. Shen, G.B. Li, S.S. Kong, D.D. Bi, S.H. Pan, B.L. Cheng, Role of piwi-interacting RNA-651 in the carcinogenesis of non-small cell lung cancer, Oncol. Lett. 15 (2018) 940–946.

[17] L. Peng, L. Song, C. Liu, X. Lv, X. Li, J. Jie, D. Zhao, D. Li, piR-55490 inhibits the growth of lung carcinoma by suppressing mTOR signaling, Tumour Biol. 37 (2016) 2749–2756.

[18] C. Le Cornet, J. Lortet-Tieulent, D. Forman, R. Beranger, A. Flechon, B. Fervers, J. Schuz, F. Bray, Testicular cancer incidence to rise by 25% by 2025 in Europe? Model-based predictions in 40 countries using population-based registry data, Eur. J. Cancer 50 (2014) 831–839.

[19] R.L. Siegel, K.D. Miller, A. Jemal, Cancer statistics, 2018, CA A Cancer J. Clin. 68 (2018) 7–30.

[20] A.A. Ghazarian, S.P. Kelly, S.F. Altekruse, P.S. Rosenberg, K.A. McGlynn, Future of testicular germ cell tumor incidence in the United States: forecast through 2026, Cancer 123 (2017) 2320–2328.

[21] N. Sedaghat, M. Fathy, M.H. Modarressi, A. Shojaie, Identifying functional cancer-specific miRNA-mRNA interactions in testicular germ cell tumor, J. Theor. Biol. 404 (2016) 82–96.

[22] B.F. Chen, Y.K. Suen, S. Gu, L. Li, W.Y. Chan, A miR-199a/miR-214 self-regulatory network via PSMD10, TP53 and DNMT1 in testicular germ cell tumor, Sci. Rep. 4 (2014) 6413.

[23] W.P. Tarrant, B.A. Czerniak, C.C. Guo, Relationship between primary and metastatic testicular germ cell tumors: a clinicopathologic analysis of 100 cases, Hum. Pathol. 44 (2013) 2220–2226.

[24] K. Iida, T. Naiki, N. Kawai, R. Ando, T. Etani, K. Tozawa, K. Kohri, Metastasectomy as optimal treatment for late relapsing solitary brain metastasis from testicular germ cell tumor: a case report, BMC Res. Notes 7 (2014) 865.

[25] O. Rascol, J. Ferreira, L. Negre-Pages, S. Perez-Lloret, L. Lacomblez, M. Galitzky, J. C. Lemarie, J.C. Corvol, J.M. Brotchie, L. Bossi, A proof-of-concept, randomized, placebo-controlled, multiple cross-overs (n-of-1) study of naftazone in Parkinson's disease, Fundam. Clin. Pharmacol. 26 (2012) 557–564.

[26] N.G. Cost, M. Adibi, J.D. Lubahn, A. Romman, G.V. Raj, A.I. Sagalowsky, V. Margulis, Effect of testicular germ cell tumor therapy on renal function, Urology 80 (2012) 641–648.

[27] C. Turnbull, E.A. Rapley, S. Seal, D. Pernet, A. Renwick, D. Hughes, M. Ricketts, R. Linger, J. Nsengimana, P. Deloukas, R.A. Huddart, D.T. Bishop, D.F. Easton, M. R. Stratton, N. Rahman, U.K.T.C. Collaboration, Variants near DMRT1, TERT and ATF7IP are associated with testicular germ cell cancer, Nat. Genet. 42 (2010) 604–607.

[28] L.H. Looijenga, H. Stoop, K. Biermann, Testicular cancer: biology and biomarkers, Virchows Arch. 464 (2014) 301–313.

[29] E.A. Rapley, G.P. Crockford, D. Teare, P. Biggs, S. Seal, R. Barfoot, S. Edwards, R. Hamoudi, K. Heimdal, S.D. Fossa, K. Tucker, J. Donald, F. Collins, M. Friedlander, D. Hogg, P. Goss, A. Heidenreich, W. Ormiston, P.A. Daly, D. Forman, T.D. Oliver, M. Leahy, R. Huddart, C.S. Cooper, J.G. Bodmer, D.

[30] G.A. Calin, C.M. Croce, MicroRNA-cancer connection: the beginning of a new tale, Cancer Res. 66 (2006) 7390–7394.

[31] K.P. Dieckmann, A. Radtke, L. Geczi, C. Matthies, P. Anheuser, U. Eckardt, J. Sommer, F. Zengerling, E. Trenti, R. Pichler, H. Belz, S. Zastrow, A. Winter, S. Melchior, J. Hammel, J. Kranz, M. Bolten, S. Krege, B. Haben, W. Loidl, C.G. Ruf, J. Heinzelbecker, A. Heidenreich, J.F. Cremers, C. Oing, T. Hermanns, C. D. Fankhauser, S. Gillessen, H. Reichegger, R. Cathomas, M. Pichler, M. Hentrich, K. Eredics, A. Lorch, C. Wulfing, S. Peine, W. Wosniok, C. Bokemeyer, G. Belge, Serum levels of MicroRNA-371a-3p (M371 test) as a new biomarker of testicular germ cell tumors: results of a prospective multicentric study, J. Clin. Oncol. 37 (2019) 1412–1423.

[32] F. Wang, Q. Wang, B. Liu, L. Mei, S. Ma, S. Wang, R. Wang, Y. Zhang, C. Niu, Z. Xiong, Y. Zheng, Z. Zhang, J. Shi, X. Song, The long noncoding RNA Synage regulates synapse stability and neuronal function in the cerebellum, Cell Death Differ. 28 (2021) 2634–2650.

[33] L.G. Rodriguez, X. Wu, J.L. Guan, Wound-healing assay, Methods Mol. Biol. 294 (2005) 23–29.

[34] A. Lal, M.P. Thomas, G. Altschuler, F. Navarro, E. O'Day, X.L. Li, C. Concepcion, Y. C. Han, J. Thiery, D.K. Rajani, A. Deutsch, O. Hofmann, A. Ventura, W. Hide, J. Lieberman, Capture of microRNA-bound mRNAs identifies the tumor suppressor miR-34a as a regulator of growth factor signaling, PLoS Genet. 7 (2011), e1002363.

[35] D. Kim, B. Langmead, S.L. Salzberg, HISAT: a fast spliced aligner with low memory requirements, Nat. Methods 12 (2015) 357–360.

[36] H. Li, B. Handsaker, A. Wysoker, T. Fennell, J. Ruan, N. Homer, G. Marth, G. Abecasis, R. Durbin, S. Genome Project Data Processing, The sequence alignment/map format and SAMtools, Bioinformatics 25 (2009) 2078–2079.

[37] Y. Liao, G.K. Smyth, W. Shi, featureCounts: an efficient general purpose program for assigning sequence reads to genomic features, Bioinformatics 30 (2014) 923–930.

[38] M.I. Love, W. Huber, S. Anders, Moderated estimation of fold change and dispersion for RNA-seq data with DESeq2, Genome Biol. 15 (2014) 550.

[39] A. Hafner, M.L. Bulyk, A. Jambhekar, G. Lahav, The multiple mechanisms that regulate p53 activity and cell fate, Nat. Rev. Mol. Cell Biol. 20 (2019) 199–210.

[40] W.S. El-Deiry, p21(WAF1) mediates cell-cycle inhibition, relevant to cancer suppression and therapy, Cancer Res. 76 (2016) 5189–5191.

[41] L. Jia, T. Wang, G. Ding, X. Kuai, X. Wang, B. Wang, W. Zhao, Y. Zhao, Trop2 inhibition of P16 expression and the cell cycle promotes intracellular calcium release in OSCC, Int. J. Biol. Macromol. 164 (2020) 2409–2417.

[42] S. Nagata, Apoptosis and clearance of apoptotic cells, Annu. Rev. Immunol. 36 (2018) 489–517.

[43] A. Ashkenazi, W.J. Fairbrother, J.D. Leverson, A.J. Souers, From basic apoptosis discoveries to advanced selective BCL-2 family inhibitors, Nat. Rev. Drug Discov. 16 (2017) 273–284.

[44] M. Sauer, S.A. Juranek, J. Marks, A. De Magis, H.G. Kazemier, D. Hilbig, D. Benhalevy, X. Wang, M. Hafner, K. Paeschke, DHX36 prevents the accumulation of translationally inactive mRNAs with G4-structures in untranslated regions, Nat. Commun. 10 (2019) 2421.

[45] Z. Yan, H.Y. Hu, X. Jiang, V. Maierhofer, E. Neb, L. He, Y. Hu, H. Hu, N. Li, W. Chen, P. Khaitovich, Widespread expression of piRNA-like molecules in somatic tissues, Nucleic Acids Res. 39 (2011) 6596–6607.

[46] V.D. Martinez, E.A. Vucic, K.L. Thu, R. Hubaux, K.S. Enfield, L.A. Pikor, D. D. Becker-Santos, C.J. Brown, S. Lam, W.L. Lam, Unique somatic and malignant expression patterns implicate PIWI-interacting RNAs in cancer-type specific biology, Sci. Rep. 5 (2015), 10423.

[47] D. Mai, P. Ding, L. Tan, J. Zhang, Z. Pan, R. Bai, C. Li, M. Li, Y. Zhou, W. Tan, Z. Zhou, Y. Li, A. Zhou, Y. Ye, L. Pan, Y. Zheng, J. Su, Z. Zuo, Z. Liu, Q. Zhao, X. Li, X. Huang, W. Li, S. Wang, B. Zou, C. Wu, R.H. Xu, J. Zheng, D. Lin, PIWI-interacting RNA-54265 is oncogenic and a potential therapeutic target in colorectal adenocarcinoma, Theranostics 8 (2018) 5213–5230.

[48] H. Han, G. Fan, S. Song, Y. Jiang, C. Qian, W. Zhang, Q. Su, X. Xue, W. Zhuang, B. Li, piRNA-30473 contributes to tumorigenesis and poor prognosis by regulating m6A RNA methylation in DLBCL, Blood 137 (2021) 1603–1614.

[49] P. Fagone, G. Nunnari, F. Lazzara, A. Longo, D. Cambria, G. Distefano, M. Palumbo, F. Nicoletti, L. Malaguarnera, M. Di Rosa, Induction of OAS gene family in HIV monocyte infected patients with high and low viral load, Antivir. Res. 131 (2016) 66–73.

[50] D.C. Hancks, M.K. Hartley, C. Hagan, N.L. Clark, N.C. Elde, Overlapping patterns of rapid evolution in the nucleic acid sensors cGAS and OAS1 suggest a common mechanism of pathogen antagonism and escape, PLoS Genet. 11 (2015), e1005203.

[51] Y. Zhang, C. Yu, Prognostic characterization of OAS1/OAS2/OAS3/OASL in breast cancer, BMC Cancer 20 (2020) 575.

[52] J.C. Kim, Y.J. Ha, K.H. Tak, S.A. Roh, Y.H. Kwon, C.W. Kim, Y.S. Yoon, J.L. Lee, Y. Park, S.K. Kim, S.Y. Kim, D.H. Cho, Y.S. Kim, Opposite functions of GSN and OAS2 on colorectal cancer metastasis, mediating perineural and lymphovascular invasion, respectively, PLoS One 13 (2018), e0202856.

[53] M. Dan, M. Zheng, L.L. Field, V. Bonnevie-Nielsen, Induction and activation of antiviral enzyme 2',5'-oligoadenylate synthetase by in vitro transcribed insulin mRNA and other cellular RNAs, Mol. Biol. Rep. 39 (2012) 7813–7822.

[54] M.R. Doherty, H. Cheon, D.J. Junk, S. Vinayak, V. Varadan, M.L. Telli, J.M. Ford, G.R. Stark, M.W. Jackson, Interferon-beta represses cancer stem cell properties in triple-negative breast cancer, Proc. Natl. Acad. Sci. U. S. A. 114 (2017) 13792–13797.

[55] B.S. Parker, J. Rautela, P.J. Hertzog, Antitumour actions of interferons: implications for cancer therapy, Nat. Rev. Cancer 16 (2016) 131–144.

[56] P. Dai, X. Wang, L.T. Gou, Z.T. Li, Z. Wen, Z.G. Chen, M.M. Hua, A. Zhong, L. Wang, H. Su, H. Wan, K. Qian, L. Liao, J. Li, B. Tian, D. Li, X.D. Fu, H.J. Shi, Y. Zhou, M.F. Liu, A translation-activating function of MIWI/piRNA during mouse spermiogenesis, Cell 179 (2019) 1566–1581, e1516.

[57] H. Tran, M. Schilling, C. Wirbelauer, D. Hess, Y. Nagamine, Facilitation of mRNA deadenylation and decay by the exosome-bound, DExH protein RHAU, Mol. Cell 13 (2004) 101–111.

[58] M.A. Hausburg, J.D. Doles, S.L. Clement, A.B. Cadwallader, M.N. Hall, P. J. Blackshear, J. Lykke-Andersen, B.B. Olwin, Post-transcriptional regulation of satellite cell quiescence by TTP-mediated mRNA decay, Elife 4 (2015), e03390.

[59] X. Chen, J. Yuan, G. Xue, S. Campanario, D. Wang, W. Wang, X. Mou, S.W. Liew, M. I. Umar, J. Isern, Y. Zhao, L. He, Y. Li, C.J. Mann, X. Yu, L. Wang, E. Perdiguero, W. Chen, Y. Xue, Y. Nagamine, C.K. Kwok, H. Sun, P. Munoz-Canoves, H. Wang, Translational control by DHX36 binding to 5′UTR G-quadruplex is essential for muscle stem-cell regenerative functions, Nat. Commun. 12 (2021) 5043.

[60] J. Nie, M. Jiang, X. Zhang, H. Tang, H. Jin, X. Huang, B. Yuan, C. Zhang, J.C. Lai, Y. Nagamine, D. Pan, W. Wang, Z. Yang, Post-transcriptional regulation of Nkx2-5 by RHAU in heart development, Cell Rep. 13 (2015) 723–732.

[61] Y. Zeng, T. Qin, V. Flamini, C. Tan, X. Zhang, Y. Cong, E. Birkin, W.G. Jiang, H. Yao, Y. Cui, Identification of DHX36 as a tumour suppressor through modulating the activities of the stress-associated proteins and cyclin-dependent kinases in breast cancer, Am. J. Cancer Res. 10 (2020) 4211–4233.

[62] Y. Cui, Z. Li, J. Cao, J. Lane, E. Birkin, X. Dong, L. Zhang, W.G. Jiang, The G4 resolvase DHX36 possesses a prognosis significance and exerts tumour suppressing function through multiple causal regulations in non-small cell lung cancer, Front. Oncol. 11 (2021), 655757.